Laser-induced pit formation in UV-antireflective coatings

Paschel, S., Balasa, I., Jensen, L., Cheng, X., Wang, Z., et al.

S. Paschel, I. Balasa, L. O. Jensen, X. Cheng, Z. Wang, D. Ristau, "Laser-induced pit formation in UV-antireflective coatings," Proc. SPIE 10805, Laser-Induced Damage in Optical Materials 2018: 50th Anniversary Conference, 108051N (16 November 2018); doi: 10.1117/12.2500338

SPIE.

Event: SPIE Laser Damage, 2018, Boulder, Colorado, United States

Laser-induced pit formation in UV-antireflective coatings

S. Paschel*[a], I. Balasa[a], L. O. Jensen[a], X. Cheng[c,d], Z. Wang[c,d], D. Ristau[a,b]

[a]Laser Zentrum Hannover e.V., Laser Components Department, Hollerithallee 8, 30419 Hanover, Germany
[b]Leibniz Universität Hannover, Institute of Quantum Optics, Welfengarten 1, 30167 Hanover, Germany
[c]MOE, Key laboratory of advanced micro-structure materials, Shanghai, 200092, China
[d]Institute of Precision Optical Engineering, School of physics science and engineering, Tongji University, Shanghai, 200092, China

ABSTRACT

Previous studies have shown that nanometer scale defects can lead to the formation of submicrometer craters, if located in coatings with a relatively small thickness. Due to the small size, such damages are challenging to detect in the online and offline damage detection and may therefore lead to an overestimation of the LIDT for the tested optical component. However, the influence of these nanopits on the optical properties and the impact on the initiation of catastrophic damage was not investigated in detail in the past. In order to study the correlation between nanopits, optical properties and catastrophic damage, samples with an AR-coating were fabricated by means of ion beam sputtering (IBS) and tested for their laser resistance by LIDT raster scans in the nanosecond regime at 355 nm. The generation and morphology changes of the nanopits were monitored for different pulse numbers and in dependence of the starting fluence. In addition to the inspection with an optical microscope in differential interference contrast (DIC) mode as prescribed by ISO 21254, alternative inspection methods, for example, dark field microscopy and scanning electron microscopy (SEM), were used to detect the nanopits. The damage test revealed that nanopits occur rarely in standard AR-coatings and possess only a small relevance for the LIDT. The typical damage morphology observed consisted of micrometer-sized pits which exhibited a stable size over a large fluence range and no growth after repeated irradiation.

Keywords: Defect-induced laser damage, nanosecond time scale, pit formation, catastrophic damage

1. INTRODUCTION

Laser-induced damage in the nanosecond regime is strongly correlated to defects, such as nanometer-sized particles, voids and stoichiometric deficiencies. Thin antireflective coatings often exhibit haze-like laser-induced damages that consist of numerous pits. Papernov et al. demonstrated that the size of pits initiated by gold nanoparticles is correlated to the depths in the coating and the initiation fluence[1]. It has been shown in a recent study about the influence of the coating thickness on the laser-induced damage threshold (LIDT) that the formation of submicrometer pits, which can be invisible in the standard damage inspection with an optical microscope, is possible[2]. Furthermore, the initiation fluence needed for the formation of such pits is significantly smaller compared to the fluence responsible for catastrophic damage. However, detailed investigations about the growth behavior of such pits and their influence on the catastrophic damage after multiple pulses were not conducted in the past due to their small size. In the case of significant pit growth up to catastrophic damage, an inspection with optical microscopy as prescribed by the ISO 21454 would not be sufficient for the determination of the LIDT and scanning electron microscopy (SEM) would be necessary.

This study is dedicated to the investigation of the initiation of nanometer-sized laser-induced pits as well as their growth behavior and morphology changes occurring after irradiation with multiple pulses for fixed fluences. Thin antireflective coatings were produced and tested regarding their laser handling capability. Line raster scans were performed on the samples due to the unknown defect distribution. The evaluation of the damage tests was realized using optical and scanning electron microscopy.

*s.paschel@lzh.de; phone 49 511 2788 484; fax 49 511 2788 100;

Laser-Induced Damage in Optical Materials 2018: 50th Anniversary Conference, edited by Christopher Wren Carr, Gregory J. Exarhos, Vitaly E. Gruzdev, Detlev Ristau, M.J. Soileau, Proc. of SPIE Vol. 10805, 108051N
 · doi: 10.1117/12.2500338

2. SAMPLE SET AND MEASUREMENT PROCEDURE

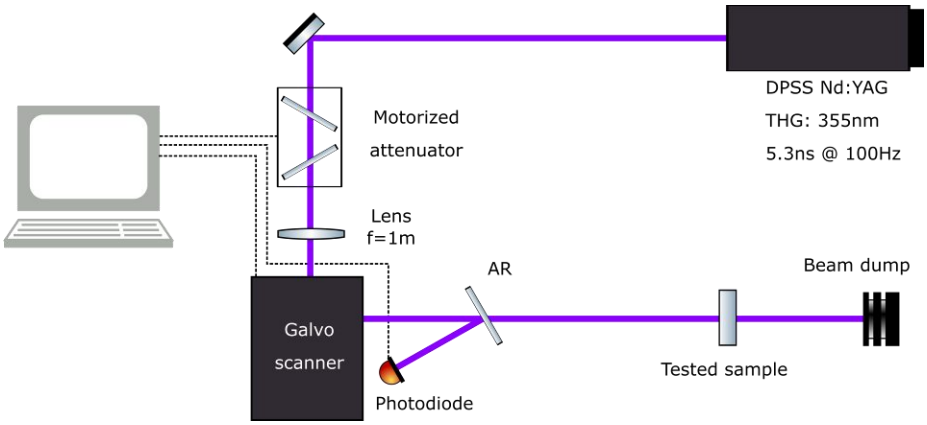

Figure 1: Schematic of the measurement setup. A DPSS Nd:YAG laser converted to the third harmonic of 355nm was used for the LIDT test. The samples were raster scanned using a galvo scanner.

A set of single side antireflective coated samples for 355 nm were fabricated by means of ion beam sputtering (IBS). All used fused silica substrates were cleaned together using a multiple stage ultrasonic cleaning system, placed on only one radius of the substrate holder and produced in the same coating run to achieve a high comparability. Post-coating annealing was performed at 300°C for 8 hours. The thin film design consisted of four layers with a total coating thickness of approximately 213 nm. The coating materials were alumina and silica.

A schematic of the measurement setup is shown in Figure 1. The LIDT measurements were performed with the SpitLight DPSS, a Nd:YAG diode pumped solid state laser from the manufacturer InnoLas Laser GmbH, operating at 355 nm with a pulse duration of 5.3 ns. A Gaussian beam profile with an effective beam diameter of approximately 200 µm, corresponding to a $1/e^2$-beam diameter of approximately 280 µm, was used at a repetition rate of 100Hz. The fluence was adjusted by a motorized attenuator and monitored by a calibrated photodiode. No online damage detection was used due to the usually small scattering signal of the expected pit damages. A galvo scanner was applied to perform 1-on-1 as well as up to 100k-on-1 line raster scans on the one inch samples. The exposure pattern is illustrated in Figure 2.

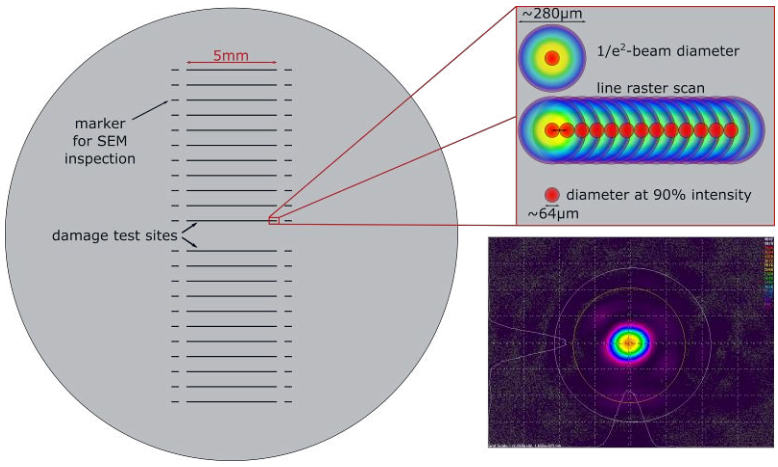

Figure 2: Exposure pattern of the test sites on the sample. Up to 22 lines of five millimeters were scanned on each sample translating the beam by the diameter at the 90% intensity of the Gaussian beam profile. Special damage markers were placed after the LIDT measurement to facilitate the offline damage detection with the SEM.

Up to 22 lines with a length of five millimeters were scanned on each one inch sample. The scanning velocity of the galvo scanner was adjusted to translate the laser spot by the beam diameter at the 90 % intensity, approx. 64 µm, of the Gaussian beam profile. The spacing between the scanned lines was set to 0.7 mm for fluences near to the damage threshold. In order to avoid contamination with debris which would falsify the results of measurements at fluences significantly exceeding the damage threshold, fewer lines were scanned increasing the spacing to 1.4 mm.
Following the line raster scans, damage markers were placed on both sides of the test sites by scanning the sample a few hundred micrometers with the highest fluence possible initiating a clearly visible damage. These markers were necessary to facilitate the offline damage inspection with a Nomarski-type microscope in differential interference contrast and dark field mode as well as a scanning electron microscope (SEM). The optical microscopy with up to 200 times magnification was applied to determine the standard damage initiation fluence whereas the scanning electron microscopy was needed to determine the initiation fluence of the nanopits and to analyze the size and morphology evolution of the occurring damages. The test samples were coated with a few nanometers of gold to avoid charging effects due to the electron beam of the SEM. A summary of the testing conditions is shown in Table 1.

Table 1: Chosen test conditions for the LIDT measurements.

Measurement procedure	1-on-1 and up to 100k-on-1 line raster scans
Wavelength	355 nm
Pulse duration	5.3 ns
Repetition rate	100 Hz
Beam profile	Gaussian
Eff. beam diameter (1/e²)	~200 µm (~280 µm)
Angle of incidence	0°
Offline damage detection	Differential interference contrast, dark field, 200x magnification Scanning electron microscopy

3. EXPERIMENTAL RESULTS

The following section discusses the results of the performed LIDT measurements. Two morphology characteristics were examined on the tested samples, the mean pit diameter and the total number of occurring pits in dependence of the initiation fluence and the number of pulses applied to the test site. SEM images of a few pits per fluence were taken and measured to determine the mean pit diameter. A LabVIEW based software was used to analyze dark field images to count the total number of pits for each scanned line by segmenting the particles from the background using a threshold for the pixel intensities.

3.1 Pit-size evolution

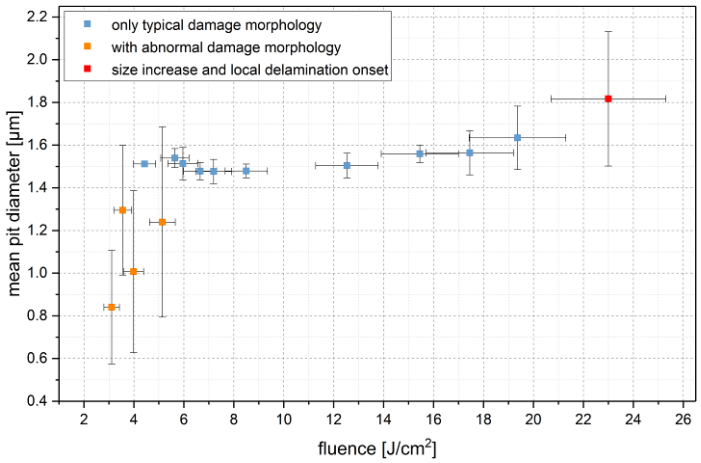

Figure 3: Shown is the mean pit diameter in dependence of the initiation fluence. A stable mean pit diameter between 1.4 µm and 1.64 µm was observed in the range of 4 J/cm² to ~20 J/cm². Submicrometer or nanopits were rarely observed.

1-on-1 measurement results of the mean pit diameter for increasing initiation fluences are shown in Figure 3 for test sample A and C. Three size ranges can be differentiated. Submicrometer damages or nanopits with arbitrary shape were rarely observed for fluences below 6 J/cm² (see Fig. 4a and 4b). The morphology of these damages, specifically the melted appearing edges, indicated an interaction with the laser pulse. However, their rare occurrence as well as their irregular shape allows no clear classification as laser-induced damage. Furthermore, other samples exhibited similar damages at much higher fluences, further supporting the approach that these abnormal damage morphologies correspond to pre-existing damages of the thin film.

Overlapping with the fluence range for the abnormal damage morphologies, fluences between 4 J/cm² and 20 J/cm² led to the initiation of flat-bottom pits as shown in Figure 4c and 4d. The mean pit diameter in this fluence range varied only slightly between 1.4 µm and 1.64 µm. All flat-bottom pits exhibited smooth outer edges indicating melting of the coating material as the dominating damage mechanism. Small scalds in the center of the pits were observed, suggesting defects and plasma formation as the initiators of the damage. Pits that occurred at higher fluences showed a change in morphology in the form of sharper inner edges, however, the pit diameter was not affected.

Further increase of the fluence up to 23 J/cm² led to the formation of micropits with a diameter of 1.82 µm (see Fig. 4e and 4f). Local delamination and indications of explosive material removal were also observed for pits close to the center of the scanned line. Catastrophic damage in the form of extensive thin film delamination was not observed at this fluence.

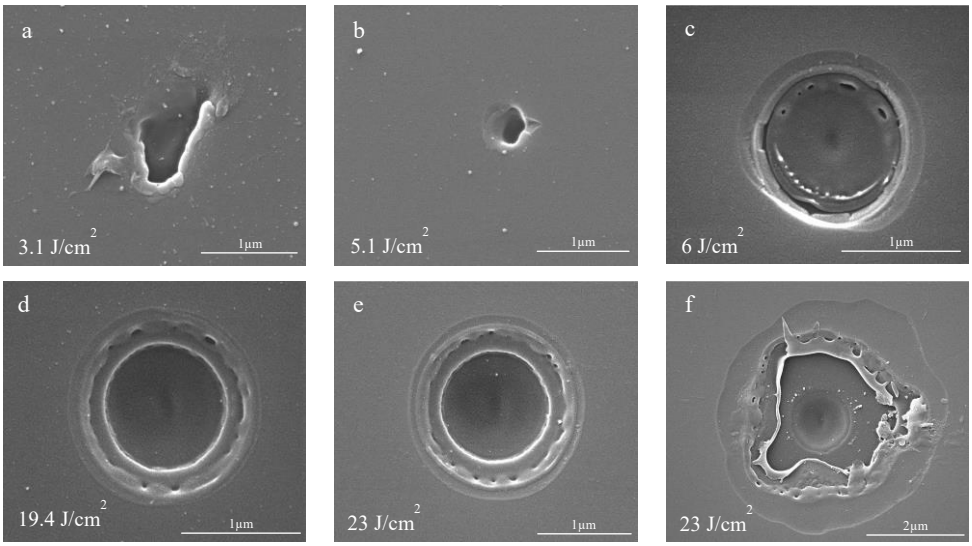

Figure 4: Damage morphologies taken with SEM. Nanopits with arbitrary shape (a, b) were rarely observed. Circular flat-bottom pits with sizes between 1.4 µm and 1.64 µm are the dominantly occurring damages (c, d). An increase of the pit diameter and local delamination around the pits was observed for a fluence of 23 J/cm² (e, f).

In order to investigate the laser durability of these pits under repeated irradiation, samples B and half of sample C were tested with S-on-1 line raster scans. The results of these measurements are shown in Figure 5. Sample B was tested with fluences of 6.4 J/cm², which was close to the damage onset. Also, 9.6 J/cm² and 13.6 J/cm² were applied, which significantly exceeded the initiation threshold. In all three cases up to 10k pulses were shot on each test site. Similar fluences were applied on sample C but with up to 100k pulses per test position. Mean pit diameters between 1.4 µm and 1.6 µm were determined for the 1-on-1 tests on Sample B and C, which is in agreement with the results of sample A. Further irradiation did neither lead to a growth of the formed micropits nor to the initiation of catastrophic damage in the form of delamination.

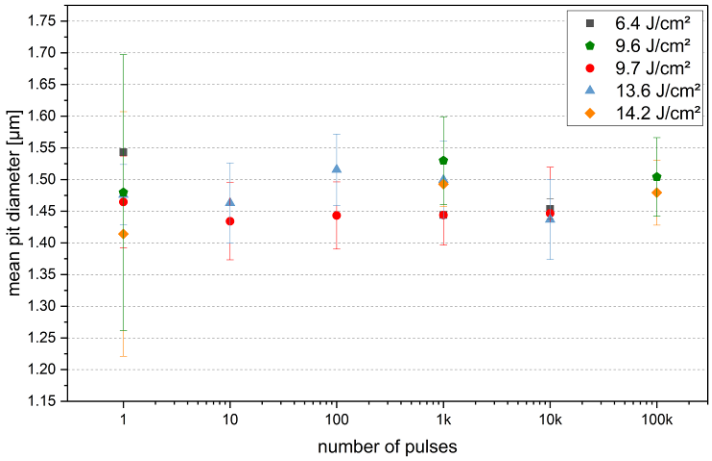

Figure 5: Mean pit diameter in dependence of the applied number of pulses. No pit growth was observed after a total amount of 100k pulses.

Typical damage morphologies of pits initiated at a fluence of 6.4J/cm², which was close to the damage onset, are shown in Figure 6a-c for different numbers of applied pulses. While all pits have an almost circular shape with sharp outer edges, it can be seen in Figure 6b, that not all material in the area of the pit is removed by the damage event. Especially the micropit after irradiation with 10k pulses shown in Figure 6c shows material that covers the scald in its center which could correspond to remelted, unremoved material.

Pictures (d-f) of Figure 6 show the damage morphology of single craters formed at a fluence of approximately 14 J/cm². The flat-bottom pits irradiated with 1 pulse (Fig. 6d) and 1k pulses (Fig. 6e) both show the same melted like edges as well as a sharp inner edge and a scald in the center. Little changes in the damage morphology can be seen after irradiation with 100k pulses as seen in Figure 6f. The micropit maintains its size and overall circular shape, however, the outer edges appear less like melted material. Furthermore, the sharp inner edge disappeared probably due to material removal by the repeated irradiation.

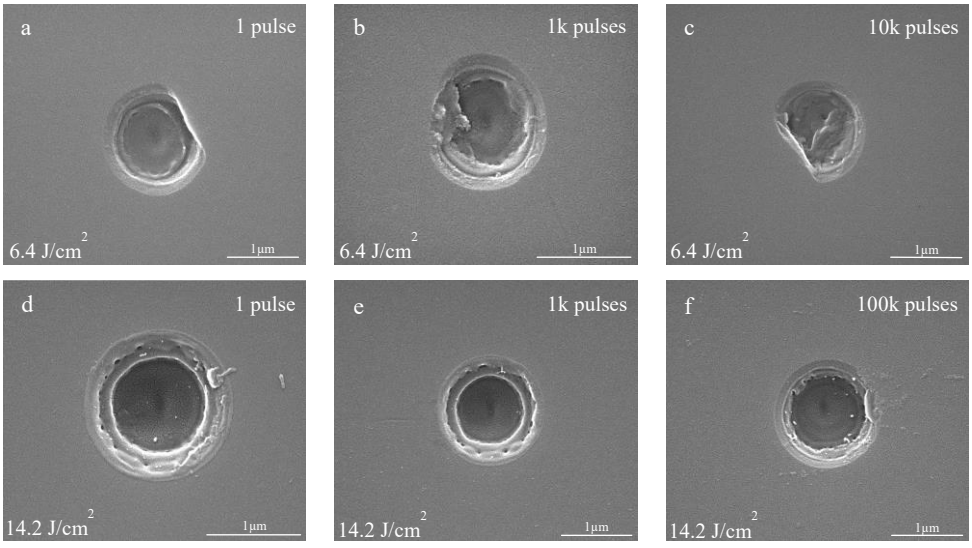

Figure 6: The top line shows SEM images of damages at 6.4J/cm² after 1 pulse (a), 1k (b) and 10k (c) pulses. The damages in the bottom line correspond to tests performed at 14.2J/cm² with 1 pulse (d), 1k (e) and 100k (f) pulses. No growth was observed for repeated irradiation at a fixed fluence, neither at the damage onset nor at more than 2 times higher fluences.

3.2 Pit-damage evolution

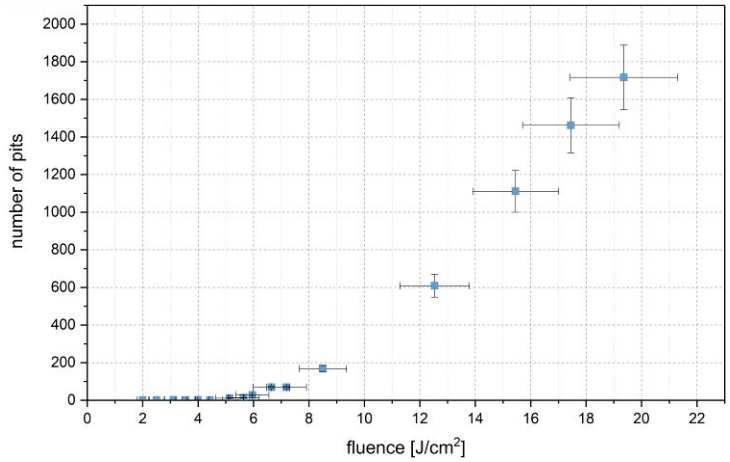

Figure 7: Total number of pits in the raster scanned line as a function of the initiation fluence.

Dark field images of the raster scanned lines on sample A were evaluated using LabVIEW based software to count the pits that occurred. The result of this evaluation is shown in Figure 7. Combination of the optical microscopy and the scanning electron microscopy resulted in an LIDT of approximately 4.5J/cm². Fluctuations of the total number of pits below this fluence value occur due to small particles with similar scattering values which are detected by the software. Near the damage onset, only a few pits are initiated in the area of 5mm x 0.2mm and the increase in pits is moderate. After 6J/cm² a strong increase in the number of pits is observed resulting in the damage structure often referred to as "gray haze" at fluences of approximately 20J/cm². This evolution of the laser-induced damage from single pits to the "gray haze" is shown in Figure 8 below.

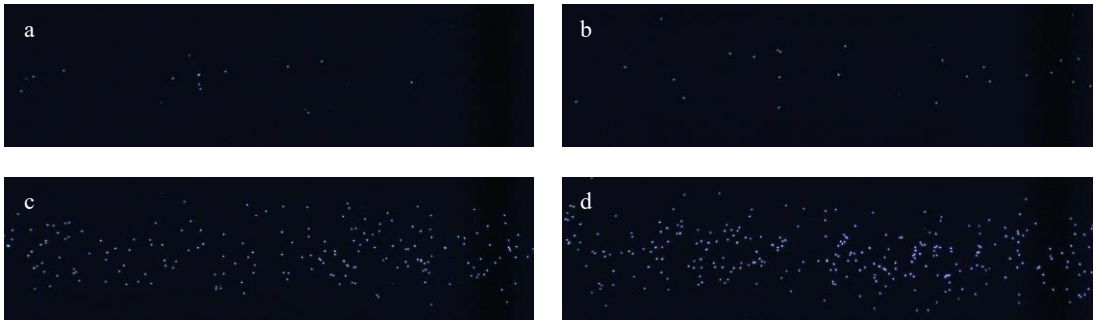

Figure 8: Evolution of the laser-induced damage from single pits to the "gray haze". Dark field images of sections of the raster scanned line for fluences of 6.7J/cm² (a), 8.5J/cm² (b), 15.5J/cm² (c), and 19.4J/cm² (d).

The tests performed on sample B with the S-on-1 procedure were used to evaluate the pulse dependent changes of the haze-like laser damage. The results are shown in Figure 9 for different fluence values. Single pulse tests on sample B are in agreement with the tests performed on sample A regarding the haze growth. However, the increase of the total number of pits is significantly smaller for sample B which indicates different defect distributions between the two samples. Increases in the number of applied pulses had no effect on the total number of micropits. Also, the occurring damages seem to be more deterministic in nature because for a fixed fluence a set amount of pits will be initiated in the area of the test.

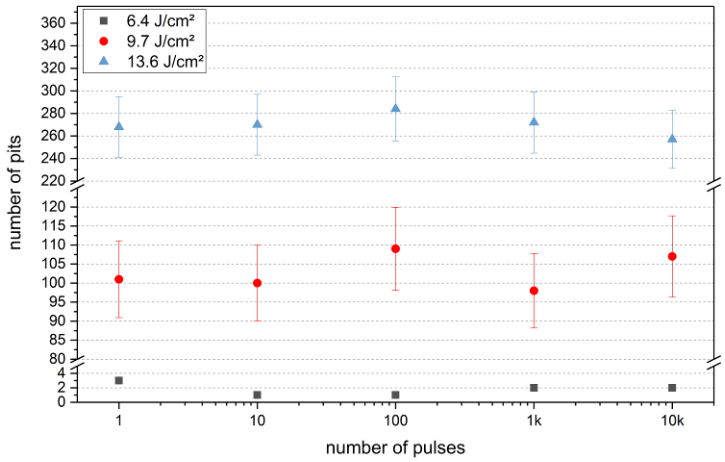

Figure 9: Total number of pits as a function of the number of pulses per test site. A set amount of pits, which is independent of the number of applied pulses, is formed for a certain fluence value.

4. CONCLUSIONS

The aim of this study was the investigation of nanometer-sized pits in order to validate their impact on the laser-induced damage threshold. In the case of growing nanopits with an impact on the catastrophic damage, on overestimation would be possible if they were not detected in the damage inspection with an optical microscope. However, the presented results of line raster scans performed on thin alumina-silica antireflective coatings at 355nm showed that nanopits occur only rarely in conventional produced thin IBS-AR-coatings. Therefore, nanopits do not seem to possess relevance in the determination of the LIDT for such optics.

The typical occurring damages were flat-bottom pits with a mean diameter of approximately 1.5µm which exhibited no growth under repeated irradiation with up to 100k pulses. Furthermore, the pit size was stable for a large fluence range starting at the damage threshold of 4.5-6J/cm² and ending at a fluence of 19.4J/cm². The collectivity of pits, also referred to as "gray haze", was independent of the number of applied pulses with a set amount of pits initiated at certain fluences. The stability of the haze-like damage as well as the stability of the micropits would allow the use of the AR-coating at fluences several times over its damage threshold if the occurring losses and influences on the pulse due to the pits are acceptable.

Further investigations are necessary in order to identify the origin of the micropits. In the current state of the study, we assume the substrate to be the limiting factor with a damage initiation by surface and subsurface damages due to the polishing method. This could be clarified by measuring the pit depth applying atomic force microscopy as well as transmission electron microscopy. Kafka et al. demonstrated the formation of nanopits in uncoated fused silica substrates depending on the polishing slurry[3], which could also be the origin for the micropits in this study. Therefore, uncoated substrates will be tested and compared regarding the pit density. Also, techniques like laser conditioning[4], chemical etching[3,5] as well as ion or plasma etching[6] could lead to an improvement of the LIDT in the case of the substrate as a limiting factor, as it was shown in other studies. Measurements of coatings with different materials are also planned in order to rule out a material dependence of the damage behavior.

ACKNOWLEDGEMENTS

This work is part of the joint research project "Visualization of Nanometer Scale Defects Responsible for Optical Loss and Laser Induced Breakdown in Binary Coating Materials for the UV Spectral Region" (GZ 1275) with the Tongji University and is funded by the Sino-German Center for Research Promotion. The funding by the Deutsche Forschungsgemeinschaft (DFG, German Research Foundation) – 317442515 and the National Natural Science Foundation of China (NSFC) is highly acknowledged.

REFERENCES

[1] S. Papernov and A. W. Schmid, "High-spatial-resolution studies of UV-laser-damage morphology in SiO2 thin films with artificial defects," Proc. SPIE 5647, Laser-Induced Damage in Optical Materials (2004).

[2] Z. Song, X. Cheng, H. Ma, J. Zhang, B. Ma, H. Jiao, and Z. Wang, "Influence of coating thickness on laser-induced damage characteristics of anti-reflection coatings irradiated by 1064 nm nanosecond laser pulses," Appl. Opt. 56, C188-C192 (2017).

[3] K. R. P. Kafka, B. Hoffman, S. Papernov, M. A. DeMarco, C. Hall, K. L. Marshall and S. G. Demos, "Methods for improving the damage performance of fused silica polished by magnetorheological finishing," Proc. SPIE 10447, Laser-Induced Damage in Optical Materials 2017, 1044709 (2017).

[4] K. R. P. Kafka, S. Papernov, and S. G. Demos, "Enhanced laser conditioning using temporally shaped pulses," Opt. Lett. 43, 1239-1242 (2018).

[5] Z. Wang, H. Yan, X. Yuan, Y. Li, K. Yang, L. Yan, L. Zhang, T. Liu and H. Li, "The effect of dynamic etching on surface quality and laser damage resistance for fused silica optics," Proc. SPIE 10173, Fourth International Symposium on Laser Interaction with Matter, 1017325 (2017).

[6] C. J. Stolz, M. D. Thomas and A. J. Griffin, "BDS thin film damage competition," Proc. SPIE 7132, Laser-Induced Damage in Optical Materials: 2008, 71320C (2008).